Available online at www.sciencedirect.com
SCIENCE DIRECT®
International Journal of Mass Spectrometry 240 (2005) 161–168
International Journal of Mass Spectrometry
www.elsevier.com/locate/ijms

Electron impact ionisation cross-sections of 2-heptanone

J.R. Vacher*, N. Blin-Simiand, F. Jorand, S. Pasquiers

Laboratoire de Physique des Gaz et des Plasmas, UMR CNRS 8578, Bât. 210, Université Paris XI, 91405 Orsay Cedex, France

Received 17 June 2004; accepted 15 October 2004
Available online 26 November 2004

Abstract

The electron impact ionisation of 2-heptanone between 13 and 78 eV is studied using mass spectrometry. $CH_3C(O)CH_2CH_2CH_2CH_2CH_3^+$ and fragment ions are produced with a total cross-section of 5×10^{-16} cm^2 towards 50 eV. Two ions, identified as CH_3CO^+ (43 amu) and $CH_3C(OH)CH_2^+$ (58 amu), contribute to about 60% of the total cross-section for electron energies above the ionisation threshold. The detected ions are identified using ab initio calculations. For $E = 14$ eV, the ion of 58 amu is the most abundant followed by an ion of 59 amu identified as being $CH_3C(OH)CH_3^+$; they result from a bond cleavage with one or two H atom rearrangements. For $E \geq 48$ eV, the ion of 43 amu is the most abundant; it results from an α-cleavage reaction in the molecular ion.
© 2004 Elsevier B.V. All rights reserved.

Keywords: Ionisation cross-section; 2-Heptanone; Mass spectrometry; VOC decomposition

1. Introduction

The 2-heptanone is an odorous molecule contained in various foods such as blue cheese. It is available for commercial use and results also from the partial oxidation of the *n*-heptane in which the oxidation at the carbon atom in position 2 predominates [1,2]. It is one of many volatile organic compounds (VOC) released in the atmosphere, contributing to the formation of pollutants, especially in urban areas. The most important tropospheric reactional pathway for this ketone is the reaction with the hydroxyl radical (OH) leading, via an H atom abstraction, to different alkyl radicals. These radicals react with O_2 to form peroxy radicals, ozone and organic nitrates by reactions with NO. The rate constant of the reaction of the OH radical with 2-heptanone has been measured [3,4], the mechanisms and the products of the different reactions have been described by Atkinson et al. [5].

These species are particularly harmful for the environment and so more and more restrictive legislations have been adopted. In Europe, the Göteborg protocol (1999) stipulates that the VOCs released in the atmosphere have to be reduced by 35% before 2010. It has been shown that the combination of a pulsed electrical discharge with a catalyst is very promising for atmospheric pollutant removal [6,7]. Experiments on 2-heptanone removal using a plasma-catalytic hybrid reactor have been performed by Ayrault et al. [8] and a high synergy effect between the oxidation catalyst used and the non-thermal plasma has been evidenced. A complete understanding of the physical and chemical mechanisms involved requires a detailed knowledge of the 2-heptanone conversion kinetics in the gas phase. Data are needed concerning the electron collision processes on the pollutant molecule, i.e., the values of the cross-sections and the types of ionic and neutral species formed via the dissociative excitation and ionisation processes. A great variety of species should be produced; they can react together through charge transfer or with oxygen atoms and with hydroxyl radicals produced by electron collisions on the background gases of the polluted effluents, i.e., O_2 and H_2O. In order to get an insight into the gas phase reactivity, kinetic models are currently being developed to predict the conversion of VOCs and the formation of by-products in the plasma. However, for the 2-heptanone, very little is known about the electron collision processes.

* Corresponding author. Tel.: +33 169 157 497; fax: +33 169 1578 44.
E-mail address: jean-rene.vacher@pgp.u-psud.fr (J.R. Vacher).

1387-3806/$ – see front matter © 2004 Elsevier B.V. All rights reserved.
doi:10.1016/j.ijms.2004.10.017

In this paper, mass spectrometry measurements of the electron impact ionisation of 2-heptanone are reported, and cross-sections for the formation of fragment ions are measured. Partition processes leading to the observed ions are suggested. We hope that these results will provide a better knowledge of the chemistry of the 2-heptanone cation, which already constitutes a rich area of research in organic mass spectrometry [9].

2. Experimental and theoretical method

The experimental apparatus and procedure have been previously described in detail elsewhere [10–12]. Some improvements have been made by modifying the gas mixture control, the data measurement and the vacuum system. The measurements are made with xenon which has an ionisation threshold of 12.13 eV [13], smaller than for argon (15.76 eV [13]) which was used previously. The choice of Xe rather than Ar allows the measurement of the evolution of cross-sections between 13 and 16 eV; this gives useful information on the nature of the ions. Moreover, the knowledge of the cross-sections at low energies is very useful in the development of kinetic models. The 2-heptanone (Aldrich, 98%) liquid is introduced at room temperature, through a septum, into a pumped stainless-steel reservoir (back pressure 10^{-3} Torr). The vapour thus formed is introduced into a gas container at a partial pressure of less than 1 Torr so as to prevent the condensation of the ketone. As it is important that the formation of condensation droplets be avoided at cold spots, the stability of the pressure is checked before the addition of xenon (Air Liquide, 99.995%) in the gas container. Pressures are measured with a precision of 0.001 Torr; the partial pressure of xenon is twice that of 2-heptanone. The gas mixture is first admitted into a gas-holder at a controlled pressure of 0.3 Torr, and then leaked, through a 50 μm diameter hole, into the analysis chamber. To reduce water impurities, the inlet gas set-up is baked and the background pressure is as low as 10^{-8} Torr.

Ions are formed in the ionisation chamber (at a constant pressure of 5×10^{-6} Torr) by the impact of a focalised electron beam over the energy range 10–78 eV. Based on a comparison with rare gas ionisation thresholds, the accuracy of the measured electron energy is estimated to be ±0.5 eV. The ions are then accelerated, focused and mass analysed in a Ribermag R 10–10 quadrupole mass spectrometer with a resolution ($M/\Delta M$) better than 400. The various ionic species are detected by means of a channel-electron multiplier followed by a Faraday cup and the collected current then recorded by a computer (which also controls all of the set-up functions). The intensity ratios of the ionic fragments of 2-heptanone to Xe^+ ions give the cross-sections for the formation of the fragments relative to that of xenon ionisation [14], the partial pressures of 2-heptanone and of xenon being known. The choice of cross-sections given by Wetzel et al. [14] is due to more detailed values near threshold than are available for other cross-sections [15–18] given by the literature. The comparison of these results allows to estimate an uncertainty of 6% (70 eV) to 10% (15 eV) on the ionisation cross-sections of Xe; this does not involve any significant error in our measurements. Concerning the intensity ratios measurements, the background noise of the residual gas is recorded before each gas admission and is taken into account.

The transmission through the quadrupole strongly depends on the analysed masses. The transmission factor measured for several masses was found to be inversely proportional to the mass, which is common for a quadrupole mass spectrometer. The cross-section for the formation of ion of mass M from 2-heptanone is given by:

$$\sigma(M) = \sigma(\mathrm{Xe})\frac{I(M)}{I(129)}\frac{Pp(\mathrm{Xe})0.283}{Pp(2\mathrm{one})}\frac{M}{129}$$

where $I(M)$ is the measured intensity for mass M, $I(129)$ is the intensity for mass 129 uma of Xe (chosen as a reference), Pp(Xe) and Pp(2one) are the partial pressures of xenon and 2-heptanone, 0.283 is the measured fraction of xenon at mass 129 uma.

In order to estimate the precision of our results, we measured the ionisation cross-section of argon by using the above formula with Ar substituted for 2-heptanone. Between 20 and 78 eV, we found fluctuations of ±20% around the values given by Wetzel et al. [14]. Below 20 eV, our results are higher than those of Wetzel, with an error up to 30% at 17 eV.

The geometrical optimisations and the total electronic energies for all the studied molecules, radicals and ions, were performed with the 6–31G(d,p) basic set using the Hartree–Fock (HF) theory. This medium level basic set allows to compare the energies of the species. The ionisation energies were computed as being the difference between the total energies of the fully optimised neutral molecule and the corresponding radical cation. This HF ab initio method underestimates the ionisation energies by 0.1–0.8 eV [19] for the alkanes. Assuming a similar trend for the species listed in Table A.1 for which experimental data are not quite available, this method allows to choose the species having the weakest ionisation energy. It should be pointed out that the use of larger basic sets does not modify the relative energies in a significant way. All the optimised geometries corresponding to a minimum point have real frequencies. Thermodynamic gas-phase data were computed at 298.15 K and 1 atm with the use of the internal thermal energy and the absolute entropy of each species. Ab initio calculations were carried out using the Gaussian 98 series of programs [20].

3. Results and discussion

Fig. 1 shows the total ionisation cross-section of 2-heptanone over an energy range of 13–78 eV. The cross-sections for the formations of various $C_nH_mO^+$ and $C_pH_q{}^+$ ions are shown in Figs. 2–5. We estimate, according to Section 2, that the uncertainty of the given values is 20% above 20 eV and 30% below 20 eV. The total ionisation cross-section plot-

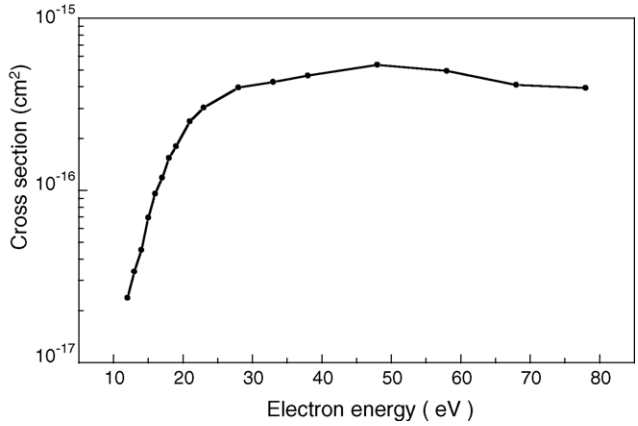

Fig. 1. Total ionisation cross-section for the formation of ions from 2-heptanone with cross-section larger than 2×10^{-18} cm^2 at 78 eV.

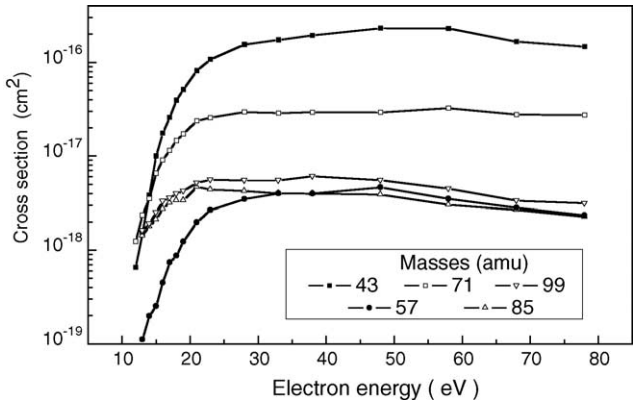

Fig. 2. Cross-section for the formation of ions issued from 2-heptanone by a simple C–C bond split.

ted in Fig. 1 is the sum of all the cross-sections listed in Table 1. As the electron impact energy increases, the total cross-section for the ion formation from 2-heptanone shows a threshold level at 10–15 eV, rising rapidly up to 30 eV and reaching a maximum value of 5×10^{-16} cm^2 at around 50 eV before decreasing slightly to 4×10^{-16} cm^2 at 78 eV, the maximum usable voltage.

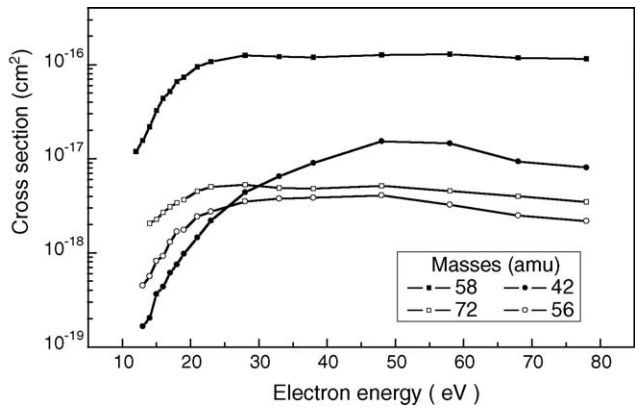

Fig. 3. Cross-section for the formation of ions issued from 2-heptanone by a C–C bond split with H atom rearrangement.

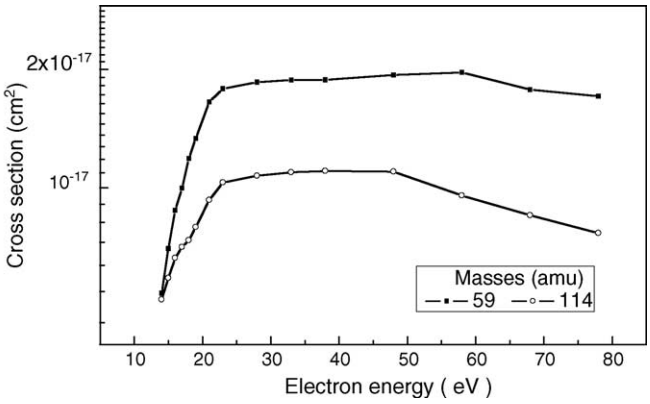

Fig. 4. Cross-section for the formation of the molecular ion and of the ion of 59 amu issued from 2-heptanone.

More than 60 different masses are observed but only 16 of them have been selected: those whose ionisation cross-section is greater than 2×10^{-18} cm^2 at 78 eV (Table 1). All the relative cross-sections are larger than 0.5% of the total cross-sections at different voltages. The first two masses in Table 1 (43 and 58 amu) contribut to about 60% of the total cross-section at this maximum voltage, a value that remains over the whole range of electron energies above the ionisation threshold. It should, however, be noticed that the most abundant ion at 78 eV (43 amu) does not remain so when energy decreases.

Discrimination effects may result from the extraction process of the ions out of the ion source and from the introduction of the ion beam into the mass analyser. This discrimination is due to the formation of some ions with an initial kinetic energy of several electron volts and with a velocity component normal to the axis of the system. This discrimination reduces the number of ions of a given mass which can be detected [21] and thus reduces the cross-section for the formation of this ion. Our experimental device does not allow the effect of this excess energy on the mass spectra to be distinguished. However, it must be pointed out that, in many cases, the prob-

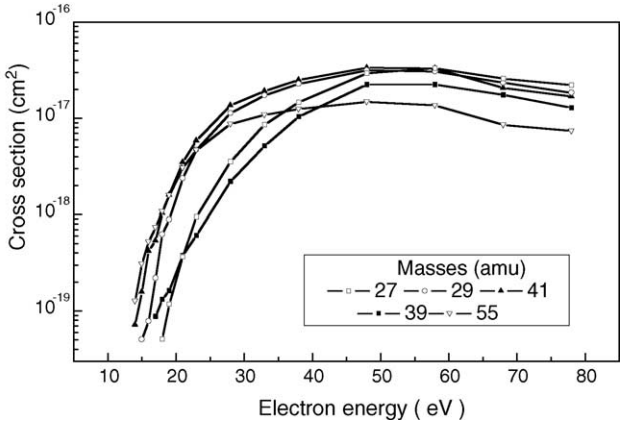

Fig. 5. Cross-section for the formation of ions of 27, 29, 39, 41 and 55 amu resulting from the dissociation of 2-heptanone.

Table 1
Cross-sections σ (10^{-16} cm^2) for the formation of the main ions from 2-heptanone at 78 eV (maximum usable voltage), 48 eV (maximum total cross-section) and two smaller voltages. Ions are listed in order of decreasing cross-section at 78 eV

Mass (amu)	78 eV		48 eV		18 eV		14 eV	
	σ	σ Relativity (%)	σ	σ Relativity (%)	σ	σ Relativity (%)	σ	σ Relativity (%)
43	1.47	36	2.32	40	0.39	24	0.039	8.2
58	1.15	28	1.29	22	0.66	41	0.22	47
71	0.27	6.6	0.29	5.0	0.15	9.2	0.035	7.4
27	0.22	5.4	0.29	5.0	–	–	–	–
29	0.18	4.4	0.32	5.5	–	–	–	–
59	0.17	4.2	0.19	3.3	0.12	7.4	0.055	12
41	0.17	4.2	0.34	5.9	0.010	0.62	–	–
39	0.13	3.2	0.22	3.8	–	–	–	–
42	0.081	2.0	0.15	2.6	0.008	2.1	–	–
114	0.077	1.9	0.11	2.0	0.074	4.6	0.052	11
55	0.073	1.8	0.15	2.6	0.059	3.6	–	–
72	0.035	0.86	0.052	0.90	0.034	2.1	0.021	4.5
99	0.031	0.76	0.055	0.95	0.039	2.4	0.019	4.0
57	0.023	0.56	0.046	0.79	0.009	0.55	–	–
85	0.023	0.56	0.039	0.67	0.034	2.1	0.019	4.0
56	0.022	0.54	0.042	0.72	0.017	1.0	0.006	1.3

ability to produce kinetically energetic ions is small. This is the case when the molecule is large and has many degrees of freedom, as for 2-heptanone, and the fragment ion's mass is large as compared to the neutral counterpart [22]. Washburn and Berry [23] have shown that for ions issued from *n*-butane, only ions of 26, 27, 39 and 41 amu undergo a significant discrimination. With 2-heptanone, we can see that the lightest ions of 27, 29, 39 and 41 amu (Fig. 5) have cross-sections around 310^{-17} cm^2; this is six times higher than for the heavier fragment ions of 85 and 99 amu (Fig. 2), which are supposed to have weaker excess kinetic energies. We can thus estimate that, for the selected masses in Table 1, no significant discriminations due to a possible excess kinetic energy occur.

All the ions listed in Table 1 have two to seven carbon atoms. The methyl ion CH_3^+ is observed at 78 eV but is very minor and disappears when the electronic energy decreases. The molecular ion $C_7H_{14}O^+$ of $M = 114$ amu and the fragment ion of 99 amu (M-15) are well observed from 78 to 13 eV. It is interesting to note that these results are different from those obtained for two alkanes having the same molecular weight M: *n*-octane [24] and iso-octane [12]. For the first alkane, the ion of M amu and the methyl ion are observed whereas the fragment ion of M-15 amu is missing. For the second one, the ion of M amu is missing whereas CH_3^+ and the fragment ion M-15 amu are observed over the whole energy range. This suggests that the formation of an appreciable number of ions from iso-octane results from primary processes: kinetic energy resulting from the electron ionising collision is converted into internal energy that can lead to the fast dissociation of the ion into a smaller one and a neutral fragment.

One must however suppose that discrimination effects due to excess kinetic energy may occur for the methyl ion. Fiegele et al. [25] have observed, using propane, that the kinetic energy distribution presents two groups of ions: one with a quasi-thermal energy and one with a kinetic energy around 3 eV. These two groups result from two different formation processes. From the kinetic energy distribution, they corrected the measured partial ionisation cross-sections for CH_3^+ by multiplying by a factor of 5.

The fact that the molecular ion is observed over the whole range of ionisation energy suggests that the formation of an appreciable number of ions results directly from the fragmentation of the molecular ion via a simple C–C bond split process or via a C–C bond split followed by a H atom rearrangement between the two fragments. The data in Figs. 2–4, with low onset energies and a rapid increase in cross-section,

Table 2
Dissociation reactions of the molecular ion ($OE^{+\bullet}$) resulting from a simple C–C bond split process and listed by increasing carbon order

$OE^{+\bullet}$			EE^+	$R^\bullet$	ΔG° (kcal mol^{-1})
(1)	$CH_3(CO)CH_2CH_2CH_2CH_2CH_3^+{}_{(114)}$	→	$C(O)CH_2CH_2CH_2CH_2CH_3^+{}_{(99)}$	$CH_{3(15)}$	+7.3
(2)	$CH_3(CO)CH_2CH_2CH_2CH_2CH_3^+{}_{(114)}$	→	$CH_3CO^+{}_{(43)}$	$CH_2CH_2CH_2CH_2CH_{3(71)}$	+14.1
(3)	$CH_3(CO)CH_2CH_2CH_2CH_2CH_3^+{}_{(114)}$	→	$CH_2CH_2CH_2CH_3^+{}_{(57)}$	$CH_3C(O)CH_{2(57)}$	+24.6
(4)	$CH_3(CO)CH_2CH_2CH_2CH_2CH_3^+{}_{(114)}$	→	$CH_3C(O)CH_2CH_2^+{}_{(71)}$	$CH_2CH_2CH_{3(43)}$	+16.0
(5)	$CH_3(CO)CH_2CH_2CH_2CH_2CH_3^+{}_{(114)}$	→	$CH_3C(O)CH_2CH_2CH_2^+{}_{(85)}$	$CH_2CH_{3(29)}$	+36.5
(6)	$CH_3(CO)CH_2CH_2CH_2CH_2CH_3^+{}_{(114)}$	→	$CH_3C(O)CH_2CH_2CH_2CH_2^+{}_{(99)}$	$CH_{3(15)}$	+34.6

Masses are given in amu.

exhibit such a formation. The data in Fig. 5 shows the cross-sections for the other ions listed in Table 1.

In the following, we will explain the formation of most of the ions considered in Table 1 as the result of a simple bond splitting of the molecular ion (Table 2) or a bond splitting with rearrangement (Table 3). We will then try to understand the nature of some of the other ions.

3.1. Formation of ions from simple bond split

The molecular ion, with one unpaired electron and an even mass number, noted $OE^{+\bullet}$ as usual, can decompose via a C–C bond cleavage, into a lighter ion with an even number of electrons and an odd mass number, noted EE^+, and an odd mass number radical noted $R^\bullet$. Table 2 lists, in order of increasing C, the six C–C bond split processes and also the masses of the corresponding ions and radicals. In such a process, not any rearrangement into the ion and the radical after the cleavage is supposed. According to Stevenson's rule, the fragment of lowest ionisation energy is favoured to retain the charge and become the ionic product; the positive charge is thus assigned with respect to the calculated ionisation energy given in Table A.1. Corresponding Gibbs energies gas phase data for dissociation reactions are computed using the previously defined theory, and are given in the right column of Table 2. These energies correspond to the difference between the total free energy of the final species in the ground state and the free energy of the initial molecular ion in the ground state. It could be possible that an activation energy is necessary for the occurrence of these splitting processes, but this is not taken into account in the present results.

Reactions (1) and (2) result from α-cleavage reactions: the oxygen atom looses a non-bonding electron during ionisation and this odd electron then forms a new bond with the adjacent C2 atom with an electron issued of one of the two adjacent bonds. An even-electron ion and a radical result from the dissociation of the molecular ion. For the ions issued from both α-cleavages, the acylium ion $CH_3C{\equiv}O^+$ (43 amu), remains the most abundant over a wide range of ionisation energies; this results from the loss of the largest alkyl radical in the molecular ion. However, the data for this ion in Fig. 2 shows that this cross-section decreases quickly below 28 eV and reaches the cross-section value for an ion of 71 amu at 14 eV and the cross-section values for ions of 85 and 99 amu at 13 eV. Two ions correspond to mass 99: the first one issued from the α-cleavage reaction (1) with loss of the C1 methyl, the second one from the bond splitting process (6) with loss of the C7 methyl. We note, according to Table 2, that reaction (1) is approximately five times less endothermic than reaction (6) and about two times less endothermic than reaction (2). Reaction (1) can thus occur with an electron energy lower than for reactions (2) and (6). At low ionisation energies, the ion of 99 amu, which has the lowest calculated ionisation energy (Table A.1), can be described as EE^+ given by reaction (1). Of course, for higher energies (above 30 eV), the two ions of 99 amu could be present.

The data for the ion of 85 amu in Fig. 2 are similar to those of 99 amu at all energies. This ion is issued from the bond dissociation (5) with loss of the terminal ethyl group. The calculated ionisation energy is close to that of the ion of 99 amu issued from reaction (6). Reactions (5) and (6) have also similar changes in the Gibbs energy. Their formation results from a similar mechanism and the cross-sections for their formation are thus similar.

The cross-sections for the formation of observed ions of 43, 57 and 71 amu below 30 eV decrease faster than for ions of 85 and 99 amu. These ions issued from reactions (2)–(4) via bond dissociation, are listed in Table 2. The Gibbs energy changes for these reactions are larger than for reactions (1) and lower than for reactions (5) and (6). The calculated ionisation energies are slightly lower than for 85 and 99 amu. Among these reactions, reaction (3) results from the migration of the charge and an inductive cleavage leading to the formation of the alkyl ion of 57 amu. As this process requires a Gibbs energy larger than for a simple bond dissociation, the cross-section for the formation of this alkyl ion is thus weak, particularly for electron energies lower than 15 eV as shown in Fig. 2.

3.2. Formation of ions from bond cleavage with rearrangement

The molecular ion, $OE^{+\bullet}$ can also be decomposed, via a C–C bond splitting and a H atom rearrangement, into a lighter ion with an odd number of electrons and even mass number ($OE^{+\bullet}$), and a neutral alkane or alkene noted *M*. Table 3 lists, according to decreasing cross-sections, the four observed ions whose formation can be described by such a mechanism. The positive charge is assigned with respect to the measured ionisation energy [13] given in Table A.2.

The ion of 58 amu (reaction 7) is the result of a two step process. First, the formation of the O–H bond occurs; this H

Table 3
Dissociation reactions of the molecular ion ($OE^{+\bullet}$) resulting from a C–C bond split with H atom rearrangement and listed in order of decreasing cross-section for 78 eV

$OE^{+\bullet}$			$OE^{+\bullet}$	M	ΔG° (kcal mol^{-1})
(7)	$CH_3(CO)CH_2CH_2CH_2CH_2CH_3^+{}_{(114)}$	→	$CH_3C(OH)CH_2^+{}_{(58)}$	$CH_2CHCH_2CH_3{}_{(56)}$	+3.0
(8)	$CH_3(CO)CH_2CH_2CH_2CH_2CH_3^+{}_{(114)}$	→	$CH_2CO^+{}_{(42)}$	$CH_3CH_2CH_2CH_2CH_3{}_{(72)}$	+17.5
(9)	$CH_3(CO)CH_2CH_2CH_2CH_2CH_3^+{}_{(114)}$	→	$CH_3C(OH)CH_2CH_2^+{}_{(72)}$	$CH_2CHCH_3{}_{(42)}$	+6.9
(10)	$CH_3(CO)CH_2CH_2CH_2CH_2CH_3^+{}_{(114)}$	→	$CH_2CH_2CO^+{}_{(56)}$	$CH_3CH_2CH_2CH_3{}_{(58)}$	+11.1

Masses are given in amu.

atom is transferred by a sterically favourable six-membered-ring transition state. It results a change in the position of the radical site now localised on the C5 atom. The second step is an α-cleavage by a splitting of the C3–C4 bond yielding the even mass ion and a stable molecule. The resonance of the radical site stabilises the product ion which is similar to an alkyl radical. This specific mechanism is well known and is usually referred to as the "McLafferty rearrangement" [26,27]. The formation of the resulting propene-2-ol ion and 1-butene is associated with a lower Gibbs energy change and reaction (7) requires a weak excess of energy. Thus, the cross-section for the formation of this ion is one of the largest over the whole ionisation energy range and is the largest for the low energies as shown in Table 1.

The ion of 42 amu can be described by the radical cation $CH_2{=}C{=}O^{+\bullet}$; it results from α-cleavage with a H atom rearrangement, before or during the C2–C3 cleavage, yielding a very stable *n*-pentane molecule. However, one can note from Fig. 3, that the cross-section for the formation of this ion clearly decreases below 50 eV. This tendency can be compared to the one observed for the ion of 57 amu in Fig. 1. Reaction (8), like reaction (3), is associated with a variation of the Gibbs energy which is appreciably higher than the previous reactions; this can thus explain the weak cross-section measured in this range of energies.

The formation of the ion of 72 amu can be described by a process similar to the formation of the ion of 58 amu with reaction (9). A H atom would be thus transferred from the C6 atom to the O radical site, then an α-cleavage reaction could initiate, from the new radical site, a C4–C5 cleavage with the loss of a propene molecule. In this process, the H atom would be transferred by a seven-membered-ring transition state and no resonance stabilisation would occur from the C4 radical site in the product ion. Jorand et al. [28] have shown that the reaction rate rearrangement via a six-membered-ring is similar to the one via a seven-membered-ring. One can moreover note from Table 3, that the Gibbs energy associated with this reaction remains low, as for reaction (7). The cross-section for the formation of this ion is approximately 1% of the total cross-section at high ionisation energy and it is 4.5% at low ionisation energy (Table 1). Therefore, the ion of 72 amu can be formed by such a mechanism.

The cross-section for the formation of the ion of 56 amu in Fig. 3 is similar to that of the ion of 72 amu for energies higher than 30 eV and becomes much smaller at weaker energies. However, this cross-section remains larger than for the ion of 42 amu and accounts for more than 1% of the total cross-section at 14 eV as shown in Table 1. If we make the assumption that this ion is formed from a cleavage and rearrangement, the Gibbs energy change associated with this formation should be included between that of reaction (8) and that of reaction (9). A C3–C4 bond splitting via a H-atom rearrangement from C1 to C4 can lead to the *n*-butane molecule and the unstable cation $CH_2C(O)CH_2^{+\bullet}$. A C atom rearrangement can then be considered through a transition by the ion cyclopropanone yielding a more stable $H_2CCH_2C{\equiv}O^{+\bullet}$ radical cation. The calculated Gibbs energy change associated to reaction (10) confirms this assumption; the ion of 56 amu could thus be produced by such a process.

The ion of 59 amu can be regarded as resulting from two H atoms rearrangements. In a first step, one H atom is transferred from the C5 atom to the O radical site. As for the ion of 58 amu, the C5 radical site can initiate an α-cleavage reaction resulting in the fragmentation of the C3–C4 bond, the fragmentation being then followed by a H atom rearrangement from the C6 to the C3 atom during the bond cleavage. This process, which is usually observed in the decomposition of esters or amides, is referred to as the "McLafferty + 1 rearrangement" [27,29]. It can lead to the $CH_3C(OH)CH_3$ cation and a 1-buten-3-yl radical:

$$CH_3C(O)CH_2CH_2CH_2CH_2CH_3^{+\bullet} \rightarrow CH_3C(OH)CH_3^{+} + C_4H_7^{\bullet} \quad (11)$$

This process is not in competition with the single H rearrangement process which remains dominant. However, the data in Table 1 shows that at 14 eV, the cross-section for the formation of the ion of 59 amu, is the largest after that of the ion of 58 amu. It is interesting to compare the cross-sections for the formation of these two ions as they are issued from the same first step of rearrangement. Figs. 3 and 4 show that the cross-sections are practically constant from 28 to 78 eV, the values for the ion of 58 amu remaining approximately six time higher than that of the ion of 59 amu. Below 28 eV, both cross-sections strongly decrease, slightly faster for the ion of 59 amu. Assuming that the common first step is relatively fast and requires a weak activation energy, the second steps are different: (i) for the ion of 58 amu, the process consists of a simple α-cleavage, (ii) for the ion of 59 amu, the migration of a H atom is necessary: this requires an additional energy and slows down the formation of this ion. The cross-section for the formation of this last ion is thus lower than that of the ion of 58 amu.

3.3. Formation of the other ions in Table 1

The cross-section for the formation of the molecular ion *M* (Fig. 4) at 78 eV is 20 times smaller than that of the predominant ion (43 amu), but it becomes larger at 14 eV (Table 1). As this predominant ion results from an α-cleavage reaction, its formation obviously requires an energy higher than 9.18 eV, the threshold for ionisation of the 2-heptanone [30]. According to the decrease of the ionisation energy, the cross-section for the ionisation of the 2-heptanone thus decreases more slowly than that of the formation of the ion of 43 amu.

Fig. 5 shows cross-sections for the formation of five ions which together account for 19% of the total cross-section at 78 eV. As the electron energy increases, the cross-sections rise relatively slowly and reach their maximum around 40–50 eV. This trend is different from what is observed (except for the ion of 42 amu) in Figs. 2–4, for which

the cross-sections remain appreciably constant beyond 30 eV. Table A.3 lists the formulas corresponding to these masses. Whereas the ions of 27 and 39 amu are identified as vinyl and propargyl ions, there is an ambiguity for the other three ions. We can observe that, with weak ionisation energies (<10 eV), these three ions have a cross-section clearly larger than that of the ion $C_2H_3^+$ and $C_3H_3^+$.

4. Conclusion

The electron impact ionisation of 2-heptanone produces molecular ions and fragment ions with a total cross-section of 5×10^{-16} cm^{-2} towards 50 eV. Cross-sections for the formation of the major species are measured between 13 and 78 eV. Two ions of 43 and 58 amu contribute to about 60% of the total cross-section at 78 eV and this trend remains the same over the whole range of electron energies above the ionisation threshold. At low energy (14 eV), ions of 58 and 59 amu are predominant and result from a bond cleavage with one or two hydrogen atoms rearrangement. The most abundant ion at high energies (≥48 eV) is the ion of 43 amu which results from a simple α-cleavage reaction in the molecular ion. The calculated ionisation energies as well as the calculated free energies of dissociation reactions of the molecular ion allow the identification of the principal observed ionic species.

Table A.1
Calculated ionisation energy for the species of Table 2

Mass	Ion	I.E. (eV)
43	CH_3CO^+	6.47
43	$CH_2CH_2CH_3^+$	7.37
71	$CH_2CH_2CH_2CH_2CH_3^+$	7.21
71	$CH_3C(O)CH_2CH_2^+$	6.42
29	$CH_2CH_3^+$	7.75
85	$CH_3C(O)CH_2CH_2CH_2^+$	7.54
15	CH_3^+	8.90
99	$CH_3C(O)CH_2CH_2CH_2CH_2^+$	7.33
99	$C(O)CH_2CH_2CH_2CH_2CH_3^+$	6.06
57	$CH_3C(O)CH_2^+$	8.23
57	$CH_2CH_2CH_2CH_3^+$	7.24

Table A.2
Ionisation energy for the species of Table 3

Mass	Ion	Name of the neutral	I.E. (eV)[a]
42	CH_2CO^+	Ketene	9.62
42	$CH_2CHCH_3^+$	Propene	9.73
72	$CH_3CH_2CH_2CH_2CH_3^+$	Pentane	10.28
72	$CH_3C(O)CH_2CH_3^+$	Butanone	9.52
58	$CH_3C(OH)CH_2^+$	Propene-2-ol	8.60
58	$CH_3CH_2CH_2CH_3^+$	Butane	10.57
56	$CH_2CH_2CO^+$	Cyclopropanone	9.10
56	$CH_2CHCH_2CH_3^+$	1-Butene	9.55

[a] From [13].

Table A.3
Possible formula and corresponding ionisation energy for the species of Fig. 5

Mass	Ion	Name of the radical	I.E. (eV)[a]
55	$C_3H_3O^+$	Propenoyl	7.00
55	$C_4H_7^+$	1-Butene-3-yl	7.49
41	C_2HO^+	Ethynyloxy	9.50
41	$C_3H_5^+$	Allyl	8.10
29	CHO^+	Formyl	8.12
29	$C_2H_5^+$	Ethyl	8.13
39	$C_3H_3^+$	Propargyl	8.67
27	$C_2H_3^+$	Vinyl	8.25

[a] From [13].

Appendix A

Supporting information available: Ionisation energies calculated for the species issued from a simple C–C bond splitting (Table A.1) and ionisation energies given by the literature (Tables A.2 and A.3).

References

[1] T.Y. Stoylkova, C.D. Chanev, H.T. Lechert, C.P. Bezouhanova, Appl. Catal. A: Gen. (2000) 203.
[2] A. Kumar, G.S. Mishra, A. Kumar, J. Mol. Catal. A: Chem. 201 (2003) 179.
[3] T.J. Wallington, M.J. Kurylo, J. Phys. Chem. 91 (1987) 5050.
[4] R. Atkinson, S.M. Aschmann, J. Phys. Chem. 92 (1988) 4008.
[5] R. Atkinson, E.C. Tuazon, S.M. Aschmann, Environ. Sci. Technol. 34 (2000) 623.
[6] T. Hammer, Plasma. Source Sci. Technol. 11 (2002) A196.
[7] K.P. Francke, H. Miessner, R. Rudolph, Catal. Today 59 (2000) 411.
[8] C. Ayrault, J. Barrault, N. Blin-Simiand, F. Jorand, S. Pasquiers, A. Rousseau, J.M. Tatibouët, Catal. Today 89 (2004) 75.
[9] G. Bouchoux, A. Luna, J. Tortajada, Int. J. Mass Spectrom. Ion Process 167/168 (1997) 353.
[10] C.V. Speller, M. Fitaire, A.M. Pointu, J. Chem. Phys. 79 (1983) 2190.
[11] J.R. Vacher, E. Le Duc, M. Fitaire, Int. J. Mass Spectrom. Ion Process 135 (1994) 139.
[12] K. Bouamra, J.R. Vacher, F. Jorand, N. Simiand, S. Pasquiers, Chem. Phys. Lett. 373 (2003) 237.
[13] NIST database, available at http://webbook.nist.gov/chemistry. Original references for data can be obtained from this database.
[14] R.C. Wetzel, F.A. Baiocchi, T.R. Hayes, R.S. Freund, Phys. Rev. A 35 (1987) 559.
[15] D. Rapp, P. Englander-Golden, J. Chem. Phys. 43 (1965) 1464.
[16] R. Rejoub, B.G. Lindsay, R.F. Stebbings, Phys. Rev. A 65 (2002) 42710.
[17] K. Stephan, T.D. Märk, J. Chem. Phys. 81 (1984) 3116.
[18] E. Krishnakumar, S.K. Srivastava, J. Phys. B 21 (1988) 1055.
[19] B.S. Jursic, J. Mol. Stuct. (Theochem.) 452 (1998) 145.
[20] Gaussian 98, Revision A.9, M.J. Frisch, G.W. Trucks, H.B. Schlegel, G.E. Scuseria, M.A. Robb, J.R. Cheeseman, V.G. Zakrzewski, J.A. Montgomery, Jr., R.E. Stratmann, J.C. Burant, S. Dapprich, J.M. Millam, A.D. Daniels, K.N. Kudin, M.C. Strain, O. Farkas, J. Tomasi, V. Barone, M. Cossi, R. Cammi, B. Mennucci, C. Pomelli, C. Adamo, S. Clifford, J. Ochterski, G.A. Petersson, P.Y. Ayala, Q. Cui, K. Morokuma, D.K. Malick, A.D. Rabuck, K. Raghavachari, J.B. Fores-

man, J. Cioslowski, J.V. Ortiz, A.G. Baboul, B.B. Stefanov, G. Liu, A. Liashenko, P. Piskorz, I. Komaromi, R. Gomperts, R.L. Martin, D.J. Fox, T. Keith, M.A. Al-Laham, C.Y. Peng, A. Nanayakkara, M. Challacombe, P.M.W. Gill, B. Johnson, W. Chen, M.W. Wong, J.L. Andres, C. Gonzalez, M. Head-Gordon, E.S. Replogle, J.A. Pople, Gaussian, Inc., Pittsburgh PA, 1998.
[21] C.E. Berry, Phys. Rev. 78 (1950) 597.
[22] C.Q. Jiao, C.A. DeJoseph Jr., A. Garscadden, J. Chem. Phys. 117 (2002) 161.
[23] H.W. Washburn, C.E. Berry, Phys. Rev. 70 (1946) 559.
[24] C.Q. Jiao, C.A. DeJoseph Jr., A. Garscadden, J. Chem. Phys. 114 (2001) 2166.
[25] T. Friegele, V. Grill, S. Matt, M. Lezius, G. Hanel, M. Probst, P. Scheier, K. Becker, H. Deutsch, O. Echt, A. Stamatovic, T.D. Märk, Vacuum 63 (2001) 561.
[26] F.W. McLafferty, Anal. Chem. 28 (1956) 306.
[27] D.G.I. Kingston, J.T. Bursey, M.M. Bursey, Chem. Rev. 74 (1974) 215.
[28] F. Jorand, A. Heiss, O. Perrin, K. Sahetchian, L. Kerhoas, J. Einhorn, Int. J. Chem. Kinet. 35 (2003) 354.
[29] F.W. McLafferty, F. Tureček, Interpretation of Mass Spectra, Fourth ed., University Science Books, Sausalito, CA, 1993.
[30] F.S. Ashmore, A.R. Burgess, J. Chem. Soc., Faraday Trans. 74 (1978) 734.